Anal. Chem. **2004,** *76,* 1507−1512

Nonequilibrium Capillary Electrophoresis of Equilibrium Mixtures, Mathematical Model

Victor Okhonin,† Svetlana M. Krylova, and Sergey N. Krylov*

Department of Chemistry, York University, Toronto, Ontario, Canada M3J 1P3

We recently introduced a new electrophoretic method, nonequilibrium capillary electrophoresis of equilibrium mixtures (NECEEM). NECEEM provides a unique way of finding kinetic and equilibrium parameters of the formation of intermolecular complexes from a single electropherogram and allows for the use of weak affinity probes in protein quantitation. In this work, we study theoretical bases of NECEEM by developing a mathematical model for the new method. By solving a system of partial differential equations with diffusion in linear approximation, we found the analytical solution for concentrations of components involved in complex formation as functions of time from the beginning of separation and position in the capillary. The nonnumerical nature of the solution makes it a powerful tool in studying the theoretical foundations of the NECEEM method and modeling experimental results. We demonstrate the use of the model for finding binding parameters of complex formation by nonlinear regression of NECEEM electropherograms obtained experimentally.

Noncovalent molecular complexes play a crucial role in regulatory biological processes, such as gene expression, DNA replication, signal transduction, cell-to-cell interaction, and the immune response. The molecular mechanisms of action of most prospective drugs are based on drugs' forming noncovalent molecular complexes with therapeutic targets.[1] In addition, the formation of noncovalent molecular complexes is pivotal to many analytical techniques and devices used in research and disease diagnostics, such as immunoassays, biosensors, and DNA hybridization analyses.[2−4]

The formation and dissociation of a noncovalent complex, C, between molecules A and B, are characterized by a bimolecular rate constant, k^+, and a unimolecular rate constant, k, of the forward and reverse reactions, respectively.

$$A + B \underset{k}{\overset{k^+}{\rightleftharpoons}} C \qquad (1)$$

The stability of the complex is often described in terms of the equilibrium dissociation constant.

$$K_d = k/k^+ \qquad (2)$$

The three constants, k^+, k, and K_d, are interconnected through eq 2; therefore, determining any pair of constants will define the third. Knowledge of the constants is essential for (i) understanding the dynamics of biological processes, (ii) determining the pharmacokinetics of target-binding drugs, and (iii) designing quantitative affinity analyses.

The methods that are used for finding k^+ and k can be divided into two broad categories: heterogeneous and homogeneous binding assays. In heterogeneous assays, A is affixed to a solid substrate, while B is dissolved in a solution and can bind A, which is affixed to the surface. In more advanced heterogeneous binding methods, such as surface plasmon resonance, A is affixed to a sensor that can change its optical or electrical signal upon B's binding to A.[5] In such methods, K_d can be found by performing a series of equilibrium experiments.[6] The concentration of B in the solution is varied, and the interaction between B and A is allowed to reach equilibrium. The signal from the sensor versus the concentration of B has a characteristic sigmoidal shape. K_d can be simply determined from the curve as the concentration of B at which the signal is equal to half of its maximum amplitude. The k value can be determined by these methods in a single nonequilibrium experiment in which the equilibrium is disturbed by quickly replacing the solution of B with a buffer devoid of B.[7] The complex on the surface dissociates in the absence of B in the solution, and the complex dissociation generates an exponential signal on the sensor.

Heterogeneous methods are relatively simple and, therefore, commonly used in binding assays. They have, however, a number of inherent drawbacks. First, affixing A to the surface changes the structure of A and, therefore, can potentially affect binding parameters of the interaction between B and A. Second, nonspecific interactions with the surface can introduce errors into binding parameters. Third, the concentration of A, which is absorbed to the surface, cannot be measured directly. Finally, heterogeneous binding assays can be time-consuming, labor-intensive, and expensive.

In homogeneous binding assays, A and B are mixed and allowed to form a complex in solution; neither of the molecules

* To whom correspondence should be addressed. E-mail: skrylov@yorku.ca.
† Permanent address: Institute of Biophysics, Siberian Branch of Russian Academy of Sciences, Krasnoyarsk, Russia 660036.

(1) Bleicher, K. H.; Böhm, H.-J.; Müller, K.; Alanine, A. I. *Nat. Rev. Drug Discovery* **2003**, *2*, 269−378.
(2) Roper, M. G.; Shackman, J. G.; Dahlgren, G. M.; Kennedy, R. T. *Anal. Chem.* **2003**, *75*, 4711−4717.
(3) Cooper, M. A. *Curr. Opin. Pharmacol.* **2003**, *3*, 557−362.
(4) Berezovski, M.; Krylov, S. N. *J. Am. Chem. Soc.* **2003**, *125*, 13451−13454.
(5) Hutter, E.; Pileni, M.-P. *J. Phys. Chem. B* **2003**, *107*, 6497−6499.
(6) Imanishi, M.; Sugiura, Y. *Biochemistry* **2002**, *41*, 1328−1334.
(7) Cheskis, B.; Freedman, L. P. *Biochemistry* **1996**, *35*, 3309−3318.

10.1021/ac035259p CCC: $27.50
Published on Web 01/22/2004

is affixed to the surface. Complex formation is followed by monitoring the changing physical−chemical properties of either A or B upon binding. Such properties can be optical (absorption, fluorescence, polarization),[8,9] or separation-related (chromatographic or electrophoretic mobility).[10,11] Equilibrium experiments with varying concentrations of B can be used similarly to heterogeneous analyses to find K_d.[8−11] Nonequilibrium stopped-flow experiments, in which A and B are mixed rapidly and the change in spectral properties is monitored, can be used to find k^+.[12,13] Nonequilibrium chromatographic experiments in which a competitive ligand is added to the chromatographic buffer and allowed to interact with A was demonstrated to be useful in finding K_d and k, although the method involved "nontransparent" numerical analysis of chromatographic peaks and required an additional reactant, the competitive ligand.[14]

When the quantity of available A or B is a limiting factor, capillary electrophoresis (CE) is the method of choice.[15] It requires only nanoliter volumes of a sample and can detect fewer than 1000 molecules.[16] Affinity capillary electrophoresis (ACE), in which A is added to the run buffer at different concentrations and the change of the mobility of B is monitored, can be used to determine K_d by conducting a series of equilibrium experiments.[17−20] However, ACE is an equilibrium approach that cannot be used for finding k.

We recently introduced a new CE-based method for finding kinetic parameters of complex formation, nonequilibrium capillary electrophoresis of equilibrium mixtures (NECEEM).[21,22] Uniquely, NECEEM allows for the determination of both k and K_d from a single electropherogram. Conceptually, the equilibrium mixture of A and B is prepared, which contains three components, A, B, and C (see eq 1). A plug of the equilibrium mixture is injected onto the capillary by pressure, and the run buffer that does not contain any of the three components is used for electrophoresis. As a result of the electrophoretic separation, the complex formation reaction is excluded from the dynamic equilibrium 1, and the complex dissociates exponentially with a unimolecular rate constant k. NECEEM electropherograms consist of peaks and exponential dissociation lines whose migration times and areas are used to calculate k and K_d. In this work, we study theoretical bases of NECEEM by developing a mathematical model of the method and applying it to fit experimental data and determine binding parameters through nonlinear regression of experimental data. The model provides adequate description of experimental NECEEM electropherograms and offers a simple and robust theoretical platform for understanding the influence of intermolecular complexes on CE electropherograms.

MATERIALS AND METHODS

Chemicals and Materials. Single-stranded DNA binding protein from *Escherichia coli* and buffer components were obtained from Sigma-Aldrich (Oakville, ON). Fluorescently labeled 15-mer DNA oligonucleotides, fluorescein-5′-GCGGAGCGTGGCAGG, was kindly donated by Dr. Yingfu Li (McMaster University, Hamilton, ON). Fused-silica capillaries were purchased from Polymicro (Phoenix, AZ). All solutions were made using Milli-Q quality deionized water and filtered through a 0.22-μm filter (Millipore, Nepean, ON).

Capillary Electrophoresis. Capillary electrophoresis analyses were performed using a Beckman-Coulter P/ACE MDQ instrument (Missisauga, ON) with on-column fluorescence detection. A 488-nm line of an Ar ion laser was utilized to excite fluorescence of the fluorescein label on the DNA molecule. An uncoated fused-silica capillary of 50 cm × 50 μm i.d. × 375 μm o.d. (effective length of 40 cm) was used. Electrophoresis was carried out with a positive electrode at the injection end biased at +30 kV, resulting in an electric field of 600 V/cm across the 50-cm-long capillary. The NECEEM run buffer was 12.5 mM sodium tetraborate at pH 9.4. The samples were injected into the capillary by a pressure pulse of 3 s × 3.5 kPa; the length and the volume of the corresponding sample plug were ∼1.7 mm and 3.3 nL, as calculated using the Poiseulle equation. The capillary was rinsed with the run buffer solution for 2 min prior to each run. At the end of each run, the capillary was rinsed with 100 mM NaOH for 2 min, followed by a rinse with deionized water for 2 min. The temperature of the capillary was maintained at 20 °C by liquid-based cooling of the capillary in all NECEEM experiments.

Equilibrium Mixtures. NECEEM experiments were performed with three different equilibrium mixtures of the single-stranded DNA-binding protein and the fluorescently labeled 15-mer DNA oligonucleotide (five repeats for every mixture). The protein and DNA were mixed in the NECEEM run buffer to have the final concentration of DNA equal to 100 nM and final concentrations of the protein equal to 0.25, 0.5, and 1 μM. The mixtures were incubated at room temperature for 1 h to reach the equilibrium prior to the analysis.

Calculations. All calculations were carried out with built-in functions in Excel software. Nonlinear regression analysis of experimental NECEEM electropherograms was performed with the Excel Solver.

RESULTS AND DISCUSSION

Major Assumptions. The goal of this study was to develop a mathematical model of NECEEM that could qualitatively and quantitatively describe experimental NECEEM electropherograms. We based our consideration on a hypothesis that solving for reaction 1 (see the introduction) under conditions of efficient

(8) Cherepanov, A. V.; De Vries, S. *Biophys. J.* **2001**, *81*, 3545−3559.
(9) DeGrazia, M. J.; Thompson, J.; Vanden Heuvel, J. P.; Peterson, B. R. *Bioorg. Med. Chem.* **2003**, *11*, 4325−4332.
(10) Wang, J.; Zhang, B.; Fang, J.; Sujino, K.; Li, H.; Otter, A.; Hindsgaul, O.; Palcic, M. M.; Wang, P. G. *J. Carbohydr. Chem.* **2003**, *22*, 347−376.
(11) Richter, S.; Cao, H.; Rana, T. M. *Biochemistry* **2002**, *41*, 6391−6397.
(12) Haas, J. A.; Fox, B. G. *Biochemistry* **2002**, *41*, 14472−14481.
(13) Jezewska, M. J.; Galletto, R.; Bujalowski, W. *J. Biol. Chem.* **2002**, *277*, 20316−20327.
(14) Avila, L. Z.; Chu, Y. H.; Blossey, E. C.; Whitesides, G. M. *J. Med. Chem.* **1993**, *36*, 126−133.
(15) Jameson, E. E.; Cunliffe, J. M.; Neubig, R. R.; Sunahara, R. K.; Kennedy, R. T. *Anal. Chem.* **2003**, *75*, 4297−4304.
(16) Wu, S.; Dovichi, N. J. *J. Chromatogr.* **1989**, *480*, 141−155.
(17) Gao, J.; Mrksich, M.; Mammen, M.; Whitesides, G. M. *High performance capillary electrophoresis: theory, techniques, and applications*; Khaledi, M. G., Ed.; John Wiley & Sons: New York, 1998; vol. 146, pp 947−972.
(18) Colton, I. J.; Carbeck, J. D.; Rao, J.; Whitesides, G. M. *Electrophoresis* **1998**, *19*, 367−382.
(19) Wan, Q.-H.; Le, X. C. *Anal. Chem.* **2000**, *72*, 5583−5589.
(20) Le, X. C.; Wan, Q.-H.; Lam, M. T. *Electrophoresis* **2002**, *23*, 903−908.
(21) Berezovski, M.; Krylov, S. N. *J. Am. Chem. Soc.* **2002**, *124*, 13674−1367.
(22) Krylov, S. N.; Berezovski, M. *Analyst* **2003**, *128*, 571−575.

electrophoretic separation of A, B, and C could provide a simple but satisfactory model. Technically, we aimed at obtaining analytical solutions for concentrations of A, B, and C in NECEEM as functions of time passed from the beginning of separation and position in the capillary. Such analytical solutions can be then used to model experimental data and determine binding parameters of complex formation. We obtained the analytical solutions under the following major assumptions.

We assume that electrophoretic zones of A and B are separated fast so that the forward reaction is negligible with respect to the reverse reaction (see reaction 1, above) during the NECEEM separation. This assumption allows us to find solutions for concentrations of A, B, and C using the linear approximation. Due to the small diameter of the capillary in comparison to its length, a one-dimensional model can be used in which the x coordinate starts in the beginning of the injection end of the capillary and codirects with its axis. The following system of partial differential equations describes mass transfer of the three components with diffusion during NECEEM:[23]

$$\frac{\partial A(t,x)}{\partial t} + v_A\frac{\partial A(t,x)}{\partial x} - \mu_A\frac{\partial^2 A(t,x)}{\partial x^2} = kC(t,x) \quad (3a)$$

$$\frac{\partial B(t,x)}{\partial t} + v_B\frac{\partial B(t,x)}{\partial x} - \mu_B\frac{\partial^2 B(t,x)}{\partial x^2} = kC(t,x) \quad (3b)$$

$$\frac{\partial C(t,x)}{\partial t} + v_C\frac{\partial C(t,x)}{\partial x} - \mu_C\frac{\partial^2 C(t,x)}{\partial x^2} = -kC(t,x) \quad (3c)$$

Here, A, B, and C are the concentrations of A, B and C, respectively; v_A, v_B, and v_C are effective velocities of A, B, and C, respectively, in electrophoresis; μ_A, μ_B, and μ_C are diffusion coefficients of A, B, and C, respectively; and k is the unimolecular constant of the dissociation of C. We assume that v_A, v_B, v_C, μ_A, μ_B, and μ_C do not change during electrophoresis.

The plug of the equilibrium mixture, which is injected into the capillary, has a length of l. We assume that the three components in the plug undergo little diffusion before the separation starts. Therefore, the initial distribution (at $t = 0$) of the components in the capillary is described by the following,

$$A(x) = A_0, \quad B(x) = B_0, \quad C(x) = C_0; \quad x \in \{0, l\}$$
$$A(x) = 0, \quad B(x) = 0, \quad C(x) = 0; \quad x \notin \{0, l\} \quad (4)$$

where A_0, B_0, and C_0 are the equilibrium concentrations of A, B, and C, respectively, in the equilibrium mixture. The solutions of differential eqs 3a−3c can be presented as integrals using the Green's function, G(t, x, v, μ, k) (Appendix 1), and initial conditions 4.

Solution for C. The solution for C is simpler than those for A and B; therefore, we find it first. The differential equation for C (see eq 3c) has a zero source function; therefore, its solution consists of a single term,

$$C(t,x) = C_0\int_0^l dx'\, G(t, x - x', v_C, \mu_C, k) = C_0\frac{\exp(-tk)}{\sqrt{2\pi}}\int_{(x-tv_C)/\sqrt{2t\mu_C}}^{(l+x-tv_C)/\sqrt{2t\mu_C}} d\gamma\, \exp(-\gamma^2/2) \quad (5)$$

where x' is the integration parameter along the length of the injected plug of the equilibrium mixture, and $\gamma = (x' - x + v_C t)/(4\mu_C t)^{1/2}$. The integral at the right-hand side of 5 can be expressed via the tabular function erf resulting in the following expression for C:

$$C(t,x) = C_0\frac{\exp(-tk)}{2}(\mathrm{erf}((l - x + tv_C)/\sqrt{4t\mu_C}) - \mathrm{erf}((tv_C - x)/\sqrt{4t\mu_C})) \quad (6)$$

Solutions for A and B. The differential equations for A and B (see eqs 3a and 3b) are similar. Therefore, their solutions will also be similar. Therefore, we find the solution for A first and then extend it to B. Equation 3a has a nonzero source function; therefore its solution is a sum of two terms.

$$A(t,x) = A_{eq}(t,x) + A_{dis}(t,x) \quad (7)$$

$A_{eq}(t, x)$ describes the migration of the electrophoretic zone of the equilibrium fraction of A. The solution for $A_{eq}(t, x)$ is found in a way similar to that for C.

$$A_{eq}(t,x) = A_0(\mathrm{erf}((l - x + tv_A)/\sqrt{4t\mu_A}) - \mathrm{erf}((tv_A - x)/\sqrt{4t\mu_A}))/2 \quad (8)$$

$A_{dis}(t, x)$ describes the migration of the electrophoretic zone of the A produced from the dissociation of C,

$$A_{dis}(t,x) = k\int_{-\infty}^{+\infty} dx'\int_0^t dt'\, G(t - t', x - x', v_A, \mu_A, 0)C(t', x') \quad (9)$$

where t' and x' are integration parameters for t and x, respectively.

If we substitute $C(t', x')$ in eq 9 with its expression through the Green's function (see eq 5), we can present A_{dis} in the following form,

$$A_{dis}(t,x) = kC_0\int_0^l dx''\int_{-\infty}^{+\infty} dx'\int_0^t dt'\, G(t - t', x - x', v_A, \mu_A, 0)G(t', x' - x'', v_C, \mu_C, k) \quad (10)$$

where x'' is the integration parameter along the length of the injected plug. Using the solution for the integral of the multiplication product of two Gauss functions (Appendix 2), we can integrate eq 10 with respect to x' and obtain,

(23) Tang, G. Y.; Yang, C.; Chai, C. J.; Gong, H. Q. *Langmuir* **2003**, *19*, 10975−10984.

$$A_{dis}(t, x) = kC_0 \int_0^l dx'' \int_0^t dt' \frac{\exp(-t'k)}{\sqrt{4\pi(\mu_C t' + \mu_A(t - t'))}} \exp\left(-\frac{(x'' + (v_C - v_A)t' - x + v_A t)^2}{4(\mu_C t' + \mu_A(t - t'))}\right) \quad (11)$$

The last integral can be solved precisely only if $\mu_C = \mu_A$. Otherwise, the approximate solution of this integral can be found using the saddle-point method. For this method to be applicable, diffusion of A and C must be slow in comparison to their translational movement (it is certainly true if A and B are large molecules, such as proteins and nucleic acids): $\mu_A t + (\mu_C - \mu_A)(x - v_A t)/(v_C - v_A) \ll (x - v_A t)^2$. We assume that the last inequality is satisfied and that $l \ll x$. With these assumptions, integral 11 can be transformed to

$$A_{dis}(t, x) \approx \frac{kC_0 \exp((x - v_A t)k/(v_C - v_A))}{(v_C - v_A)} \epsilon_A \int_0^{l/\epsilon_A} d\psi \int_{(v_A t - x)/\epsilon_A}^{(v_C t - x)/\epsilon_A} \frac{d\varphi}{\sqrt{\pi}} \exp(-(\psi + \varphi)^2) \quad (12)$$

where $\epsilon_A = 2\sqrt{(\mu_C(x - v_A t) - \mu_A(x - v_C t))/(v_C - v_A)}$, and ψ and φ are the parameters of integration linearly dependent on x'' and t', respectively.

Integral 12 can be solved through the erf functions (see Appendix 3).

$$A_{dis}(t, x) \approx \frac{kC_0 \exp((x - v_A t)k/(v_C - v_A))}{2(v_C - v_A)} \epsilon_A I(l/\epsilon_A, (v_C t - x)/\epsilon_A, (v_A t - x)/\epsilon_A) \quad (13)$$

The solution for B is similar to that for A. Accordingly, eqs 7, 8, and 13 can be modified for B,

$$B(t, x) = B_{eq}(t, x) + B_{dis}(t, x) \quad (14)$$

$$B_{eq}(t, x) = B_0(\mathrm{erf}((l - x + tv_B)/\sqrt{4t\mu_B}) - \mathrm{erf}((tv_B - x)/\sqrt{4t\mu_B}))/2 \quad (15)$$

$$B_{dis}(t, x) \approx \frac{kC_0 \exp((x - v_B t)k/(v_C - v_B))}{2(v_C - v_B)} \epsilon_B I(l/\epsilon_B, (v_C t - x)/\epsilon_B, (v_B t - x)/\epsilon_B) \quad (16)$$

where

$$\epsilon_B = 2\sqrt{(\mu_C(x - v_B t) - \mu_B(x - v_C t))/(v_C - v_B)} \quad (17)$$

The concentrations of A, B, and C for given t and x can be calculated using expressions 6, 7, 12, 13, and 14−16 and any spreadsheet-type software with built-in mathematical functions. In this work, we used the Excel program.

Simulated Electropherograms. We used eqs 6, 7, 12, 13, and 14−16, which describe $A(t, x)$, $B(t, x)$, and $C(t, x)$, to build simulated electropherograms. To be comparable with experimental electropherograms, which are typically generated with a detector placed in a fixed position on the capillary or past the capillary, we assume that x is constant. Thus, our simulated electropherograms contain solutions for concentrations as functions of t for fixed x: $A(t)$, $B(t)$, and $C(t)$. For graphical presentation, these solutions should be multiplied by the velocities of corresponding species v_A, v_B, and v_C if simulated electropherograms are to model experimental data obtained with sheath-flow-type off-column detection. The areas under the features in velocity-corrected electropherograms correspond to the amounts of separated species.

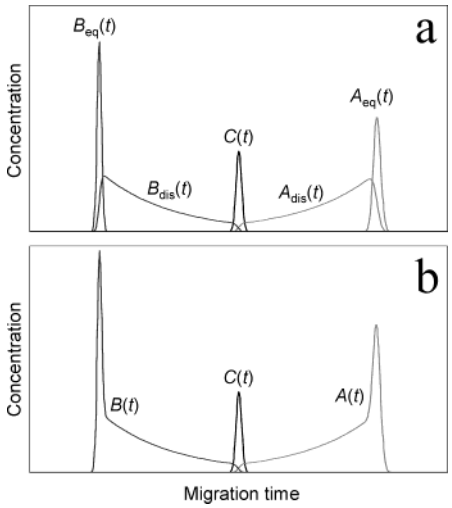

Figure 1. Simulated NECEEM electropherograms. Panel a illustrates characteristic features produced by (i) peaks $A_{eq}(t)$ and $B_{eq}(t)$ corresponding to equilibrium fractions of A and B; (ii) exponential decay lines $A_{dis}(t)$ and $B_{dis}(t)$ corresponding to A and B, produced from the dissociation of C; and (iii) peak $C(t)$ corresponding to the fractions of intact C reaching the detection point. Panel b shows simulated electrophoretic features generated by experimentally distinguishable species $A(t)$, $B(t)$, and $C(t)$.

The solution for $C(t)$ has one term (see eq 6), whereas the solutions for $A(t)$ and $B(t)$ consist of two terms, $A_{eq}(t)$ and $A_{dis}(t)$ (see eqs 7, 8, and 13) and $B_{eq}(t)$ and $B_{dis}(t)$ (see eqs 14−16), respectively. $A_{eq}(t)$, $B_{eq}(t)$, and $C(t)$ are Gaussian peaks, whereas $A_{dis}(t)$ and $B_{dis}(t)$ are lines corresponding to the production of A and B due to the dissociation of C (Figure 1a). We cannot distinguish $A_{eq}(t)$ from $A_{dis}(t)$ and $B_{eq}(t)$ from $B_{dis}(t)$ experimentally. Therefore, to be comparable with experimental electropherograms, simulated ones have to contain $A(t) = A_{eq}(t) + A_{dis}(t)$ and $B(t) = B_q(t) + B_{is}(t)$ instead of $A_{eq}(t)$, $A_{dis}(t)$, $B_{eq}(t)$, and $B_{dis}(t)$ (Figure 1b).

There are three qualitatively distinct types of simulated NECEEM electropherograms, depending on the value of the dissociation rate constant, k, with respect to the reciprocal migration time of C, $1/t_C$ (Figure 2). If $k \ll 1/t_C$, the dissociation of C is not significant, and three peaks corresponding to equilibrium fractions of A, B, and C are observed in a NECEEM electropherogram (Figure 2a). This is the simplest case, in which NECEEM is reduced to the equilibrium separation of A, B, and C. If $k \sim 1/t_C$, the dissociation of C during separation is significant, but a detectable amount of C reaches the detector. The simulated NECEEM electropherogram still contains three peaks corresponding to equilibrium fractions of A and B and the fraction of

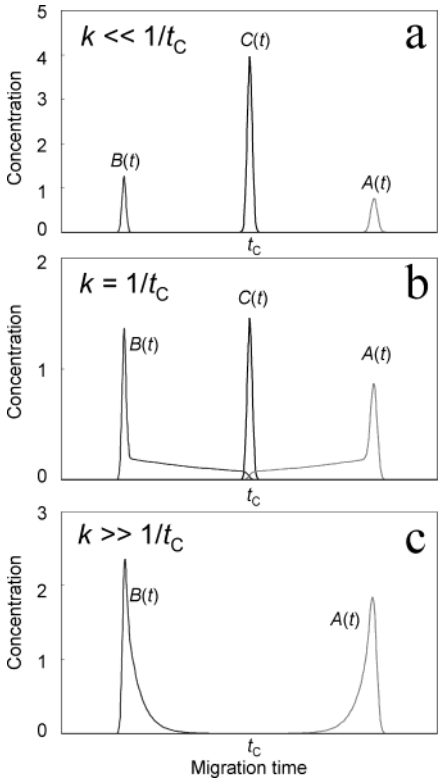

Figure 2. Simulated NECEEM electropherograms obtained for different values of the rate constant, k, of the dissociation of complex C with respect to the reciprocal migration time of C ($1/t_C$): $k \ll 1/t_C$ (panel a), $k = 1/t_C$ (panel b), and $k \gg 1/t_C$ (panel c).

intact C which reached the detector (Figure 2b). In addition to the three peaks, it contains two lines, corresponding to A and B produced from the dissociation of C. Finally, if $k \gg 1/t_C$, then C dissociates to undetectable levels, and the electropherogram does not contain peak C (Figure 2c). The extent of the dissociation can be changed by varying t_C via, for example, changing the effective length of the capillary (the distance from the injection end to the detection point) or the velocity of C, which depends on the electric field. Despite the absence of peak C, the electropherogram depicted in Figure 2c can still be used to obtain both binding parameters, k and K_d.[22] It can also be used to determine the amount of A if B is an affinity probe (or vice versa).[24]

It is worthwhile to mention that the electropherogram shown in Figure 2c suggests that tailing and fronting, which are often observed in CE, can originate from complex formation between the analyte and components of the sample matrix. If the run buffer is different from the sample buffer, the complex will be decaying during the separation, and complex decay will lead to electropherogram features similar to those in Figure 2c.

Determination of K_d and k. Simulated NECEEM electropherograms can help to understand the principles of finding binding parameters from experimental NECEEM electropherograms. By definition, the value of the equilibrium dissociation constant, K_d, can be determined from equilibrium amounts, A_{eq}, B_{eq}, and C_{eq}, of the three components in the equilibrium mixture if they all are detectable.

$$K_d = \frac{A_{eq}B_{eq}}{C_{eq}} \tag{18}$$

Alternatively, K_d can be determined from equilibrium amounts of two components if the third one is undetectable. For example, if B cannot be detected, K_d can be determined on the basis of equilibrium amounts of A (A_{eq}) and C (C_{eq}) and total concentrations of A (A_{tot}) and B (B_{tot}) mixed.

$$K_d = \frac{B_{tot}(1 + A_{eq}/C_{eq}) - A_{tot}}{1 + C_{eq}/A_{eq}} \tag{19}$$

By definition, the unimolecular rate constant of the dissociation of C can be determined if C_{eq} and the amount of C remaining intact (C_{intact}) at time t_C are known.

$$k = \frac{\ln(C_{eq}/C_{intact})}{t_C} \tag{20}$$

To find K_d and k using formulas 19 and 20 we need to determine A_{eq}/C_{eq}, C_{eq}/C_{intact}, and t_C. The three parameters can be determined precisely from a single NECEEM electropherogram if it is of the type presented in Figure 1a. Indeed, t_C is simply the migration time of C. The areas under $A_{eq}(t)$ and $B_{eq}(t)$ correspond A_{eq} and B_{eq}, respectively. The areas under $A_{dis}(t)$ and $B_{dis}(t)$ are equal due to the mass balance; therefore, both the area under $C(t) + A_{dis}(t)$ and the area under $C(t) + B_{dis}(t)$ are equal to C_{eq}. However, in the experiment, we cannot distinguish $A_{eq}(t)$ from $A_{dis}(t)$ and $B_{eq}(t)$ from $B_{dis}(t)$. This requires that such a distinction be made from an electropherogram consisting of $A(t) = A_{eq}(t) + A_{dis}(t)$ and $B(t) = B_{eq}(t) + B_{dis}(t)$ (Figure 1b**)**. The overlap between $A_{eq}(t)$ and $A_{dis}(t)$ as well as $B_{eq}(t)$ and $B_{dis}(t)$ leaves some uncertainty as to how to distinguish between them. This emphasizes the need for a more accurate way of finding A_{eq}/C_{eq} and C_{eq}/C_{intact} from NECEEM electropherograms, which would lead to unambiguous determination of K_d and k. One of the approaches to accurate finding of A_{eq}/C_{eq} is described in the following paragraph.

Here, we demonstrate that K_d and k can be found by nonlinear regression of experimental NECEEM electropherograms using the mathematical model developed. The experimental data modeled were obtained for the interaction between a fluorescently labeled 15-mer DNA oligonucleotide (A) and single-stranded DNA binding protein (B).[21,22] Due to the fluorescence label on A, both A and C were detectable, but B was not. Therefore, experimental NECEEM electropherograms contained fluorescence traces of A and C only. Nonlinear regression was based on minimizing the deviation between the experimental trace and a model function $A(t) + C(t)$ using the least-squares method. The parameters optimized in the regression analysis were k, v_A, v_C, μ_A, μ_C, and the A_{eq}/C_{eq} ratio. Thus, k was found directly from the regression procedure, whereas K_d was calculated using eq 19 with the A_{eq}/C_{eq} value found in the regression. Due to the analytical nature of the model, satisfactory fitting of one electropherogram is rapidly calculated, even with the relatively slow Excel solver. Experiments were conducted with three different sets of concentrations of A

(24) Berezovski, M.; Nutiu, R.; Li, Y.-F.; Krylov, S. N. *Anal. Chem.* **2003**, *75*, 1382−1386.

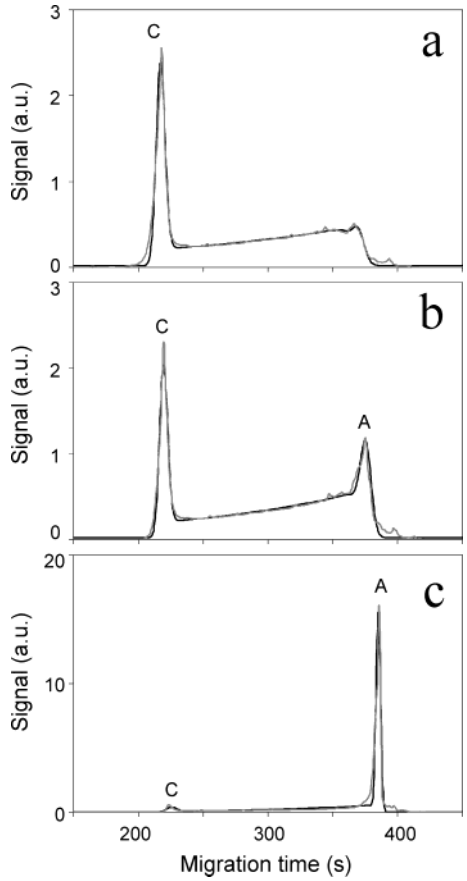

Figure 3. Fitting experimental NECEEM electropherograms with simulated ones. Experimental NECEEM electropherograms (red lines) were obtained for the interaction between a fluorescently labeled DNA 15-mer oligonucleotide (0.1 μM) and a single-stranded DNA-binding protein: 1 (panel a), 0.5 (panel b), and 0.25 μM (panel c). Simulated NECEEM electropherograms (black lines) were obtained by nonlinear regression of the experimental data using the least-squares method. A denotes the DNA, and C denotes the protein−DNA complex.

and B to generate three qualitatively different NECEEM electropherograms. The results of the regression of representative experimental data are shown in Figure 3. Binding parameters were determined by averaging those for the three sets of different experimental conditions (five repeats for every set): $k = (4.5 \pm 1.2) \times 10^{-3}$ s^{-1} and $K_d = (1.9 \pm 0.7) \times 10^{-8}$ M^{-1}s^{-1}. These values are lower than those published earlier[21,22] due to adjustments to our standard NECEEM procedure. Namely, we lowered the temperature inside the capillary and kept it constant by using a CE apparatus with a liquid-cooled capillary. In addition, to demonstrate more pronounced peaks of the complex, we used higher concentrations of the protein, at which it is known to form multimers, whose affinity to DNA is greater than that of a monomer protein.[25]

To conclude, we have developed the mathematical models of NECEEM, which provides the analytical solution for concentrations of interacting components in the linear approximation with diffusion. The model satisfactorily explains the experimental results and the origin of features (peaks, tailing, and fronting) in electropherograms obtained from samples that include dissociating complexes. The model allows for finding binding parameters, K_d and k, from a single experimental electropherogram in a fast and accurate way, providing the bases for using CE as a powerful analytical method in studies of noncovalent molecular complexes.

ACKNOWLEDGMENT

The authors thank Maxim Berezovski for technical assistance. This work was supported by an Ontario Cancer Research Network grant to S.N.K.

APPENDIX 1. GREEN'S FUNCTION

Mass transfer with diffusion is described by the following generalized equation,

$$\frac{\partial G(t, x)}{\partial t} + v\frac{\partial G(t, x)}{\partial x} - \mu\frac{\partial^2 G(t, x)}{\partial x^2} = -kG$$

where v, μ, and k are numeric parameters. If the x distribution of G at time zero is a delta function, then by definition, the solution of the above equation is the Green's function.

$$G(t, x, v, \mu, k) = \begin{cases} (\exp(-kt - (x - vt)^2/4\mu t)/\sqrt{4\pi\mu t}; & t > 0 \\ 0; & t < 0. \end{cases}$$

APPENDIX 2. INTEGRAL OF THE MULTIPLICATION PRODUCT OF TWO GAUSS FUNCTIONS

The integral of the product of two Gauss functions with infinite limits has the following solution:

$$\int_{-\infty}^{+\infty} \frac{1}{\pi\sqrt{\lambda\omega}} \exp\left(-\frac{(x - \epsilon)^2}{\lambda}\right) \times \exp\left(-\frac{(x - \eta)^2}{\omega}\right) dx = \frac{1}{\sqrt{\pi(\lambda + \omega)}} \exp\left(-\frac{(\eta - \epsilon)^2}{\lambda + \omega}\right)$$

APPENDIX 3. DOUBLE INTEGRAL OF GAUSS FUNCTION IN FINITE LIMITS

The double integral of Gauss function in finite limits has the following solution:

$$I(\chi, \psi, \theta) = \frac{2}{\sqrt{\pi}} \int_0^{\chi} d\gamma \int_{\theta}^{\psi} d\varphi \exp(-(\gamma + \varphi)^2)$$

$$= (\psi + \chi)\mathrm{erf}(\psi + \chi) - \psi\mathrm{erf}(\psi) - (\theta + \chi)\mathrm{erf}(\theta + \chi) + \theta\mathrm{erf}(\theta) + (\exp(-(\psi + \chi)^2) - \exp(-\psi^2) - \exp(-(\theta + \chi)^2) + \exp(-\theta^2))/\sqrt{\pi}$$

where

$$\mathrm{erf}(x) = \frac{2}{\sqrt{\pi}} \int_0^x \exp(-y^2)\, dy.$$

Received for review October 24, 2003. Accepted December 15, 2003.

AC035259P

(25) Bujalowski, W.; Lohman, T. M. *J. Mol. Biol.* **1991**, *217*, 63−74.